Behaviors of Self-Assembled Diblock Copolymer with Pendant Photosensitive Azobenzene Segments

JUI-HSIANG LIU, YI-HONG CHIU

Department of Chemical Engineering, National Cheng Kung University, Tainan 70101, Taiwan

Received 22 October 2009; accepted 8 December 2009
DOI: 10.1002/pola.23871

ABSTRACT: A novel monomer, ethyl 4-[4-(11-methacryloyloxyundecyloxy)phenyl azobenzoyl-oxyl] benzoate, containing a photoisomerizable N=N group was synthesized. The monomer was further diblock copolymerized with methyl methacrylate. Amphiphilic diblock copolymer poly(methyl methacrylate-*block*-ethyl 4-[4-(11-methacryloyloxyundecyloxy)phenyl azobenzoyl-oxyl] benzoate (**PMMA**-***b***-**PAzoMA**) was synthesized using atom transfer radical polymerization. The reverse micelles with spherical construction were obtained with 2 wt % of the diblock copolymer in a THF/H_2O mixture of 1:2. Under alternating UV and visible light illumination, reversible changes in micellar structure between sphere and rod-like particles took place as a result of the reversible E-Z photoisomerization of azobenzene segments in **PMMA**-***b***-**PAzoMA**. Microphase separation of the amphiphilic diblock copolymer in thin films was achieved through thermal and solvent aligning methods. The microphases of the annealed thin films were investigated using atom force microscopy topology and scanning electron microscopy analyses. © 2010 Wiley Periodicals, Inc. J Polym Sci Part A: Polym Chem 48: 1142–1148, 2010

KEYWORDS: AFM; annealing; atom transfer radical polymerization (ATRP); block copolymers; diblock copolymers; isomer/isomerization; polymers; self-assembly; thin films

---

INTRODUCTION

Block copolymers exhibit nanoscale self-assembly behavior to form microscopically ordered structures called microphases. Most block copolymers are known to exhibit a microphase separation from a disordered state to an ordered state upon cooling. The unfavorable interactions between dissimilar monomers comprising a given block copolymer are considered to be the cause for such behavior. Microphase separation (nanostructure formation) by block copolymers in thin films has been the subject of intense study because of interest in the phenomenological aspects of self-assembly in a confined state.[1–6] From a practical viewpoint, such nanostructures also received considerable attention for fabrication of even smaller feature than those obtained by the photolithography process.[7–9] Such nanostructures have potential applications in high-density data storage media,[10,11] ultrafine filters or membranes,[12] as templates for metal nanowires,[13,14] and so forth.[15]

A more recent study on small-molecule azobenzene compounds, in which the *trans–cis* photoisomerization imparts an amphiphilic character to the molecules, found that azobenzenes can display enhanced fluorescence emission in solution after a prolonged UV irradiation, as a result of light-driven molecular self-assembly into micellar aggregates. Azobenzene-containing polymers are widely studied because of their potential applications in many fields, which include optical data storage,[16] liquid crystal displays,[17] and holographic surface-relief gratings.[18] The photoresponsive properties of the polymers are based on the *trans*-to-*cis* and the *cis*-to-*trans* photoisomerizations of azobenzene, which lead to considerable changes in their molecular shape and dipole moments.[19–24]

Recent studies show that polymers containing azobenzenes (azo polymers for short) can exhibit fascinating photoresponsive variations, such as phase transition,[25,26] chromophore orientation,[27] surface-relief-grating formation,[28] and photomechanical bending.[29] The variations are triggered by the *trans–cis* photoisomerization of the azobenzenes. The isomerization behavior of the azo chromophores plays a critical role in affecting the properties of azo polymers.

In this study, a diblock copolymer (**PMMA-*b*-PAzoMA**) consisting of poly(methyl methacrylate) and azobenzene was synthesized using atom transfer radical polymerization (ATRP). Photoresponsive uniform colloidal spheres were constructed from the amphiphilic azobenzene containing diblock copolymer. Under alternating UV and visible light illumination, reversible changes in micellar structure between sphere and rod-like particles took place as a result of the reversible E-Z photoisomerization of azobenzene segments in **PMMA-*b*-PAzoMA**. Microphase separation of the amphiphilic diblock copolymer in thin films was achieved through thermal and solvent aligning methods. The morphology of the annealed thin films was investigated using atom force microscopy (AFM) topology and scanning electron microscopy (SEM) analyses.

Additional Supporting Information may be found in the online version of this article. Correspondence to: J.-H. Liu (E-mail: jhliu@mail.ncku.edu.tw)

Journal of Polymer Science: Part A: Polymer Chemistry, Vol. 48, 1142–1148 (2010) © 2010 Wiley Periodicals, Inc.

EXPERIMENTAL

Measurements

All new compounds were characterized by ^{1}H NMR, FTIR, and elemental analysis (EA). FTIR spectra were recorded with a KBr disk on a Jasco VALOR III (Tokyo, Japan) FTIR spectrophotometer. ^{1}H NMR (400 MHz) and H spectra were obtained from a Bruker AMX-400 (Darmstadt, Germany) high-resolution ^{1}H NMR spectrometer, and chemical shifts were reported in ppm with tetramethylsilane (TMS) as an internal standard. Elemental analyses were carried out on a Heraeus CHN-O (Darmstadt, Germany) rapid elemental analyzer. Gel permeation chromatography (GPC) measurements were performed at 40 °C with a Hitachi L-4200 (Osaka, Japan) instrument equipped with TSK gel GMH and G2000H columns. $CHCl_3$ was used as the eluent in these columns, with a rate of elution of 1.0 mL/min. The instrument was calibrated with a polystyrene standard. UV–vis absorption spectra were measured with a Jasco V-550 spectrophoto-meter. SEM images were taken with a JEOL HR-FESEM JSM-6700F (Osaka, Japan) instrument. The morphology of the colloidal spheres and the surface microphase separation were characterized by transmission electron microscopy (TEM) and AFM.

Materials

All chemical reagents are purchased from Tokyo Chemicals (TCI, Japan). All organic solvents were purchased from Aldrich Chemical. Analytical thin-layer chromatography is conducted on Merck aluminum plates with 0.2 mm of silica gel 60F-254.

Synthesis of Monomer

Ethyl 4-(4-Hydroxyphenylazo) Benzoate (1)

Ethyl 4-aminobenzoate (5 g, 30 mmol) was dissolved in 1 M aqueous HCl (100 mL) and kept in an ice bath at 0 °C. Sodium nitrite (3.53 g, 51.16 mmol) in water (20 mL) was added dropwise to the former solution and stirred for 30 min. Sodium hydroxide (4.4 g, 0.11 mol) and phenol (5.0 g, 53.19 mmol) were dissolved in water (100 mL) and stirred at 0 °C for 30 min. The former reaction mixture was added dropwise to the latter solution at 0 °C and then stirred for 1 h. The resulting mixture was poured into water, and the solution was neutralized with 5% aqueous HCl. The crude product of compound **1** was filtered and recrystallized twice from ethanol. M.p. = 154 °C. Yield: 47%. IR: 3615 v(—OH), 1720 (C=O), and 2120 (N=N). Analysis for ethyl 4-(4-hydroxyphenylazo) benzoate (**1**) ($C_{15}H_{14}O_3N_2$, 270): Calc.: C, 66.67; H, 5.19; N, 10.37. Found: C, 66.64; H, 5.21; N, 10.34.

Ethyl 4-[4-(6-Hydroxyundecyl)phenylazo] Benzoate (2)

Compound **1** (4.96 g, 18.4 mmol) was dissolved in ethanol (100 mL). Potassium hydroxide (1.2 g, 22.1 mmol) dissolved in ethanol (30 mL) was then added dropwise to the former solution. 11-Bromo-1-undecanol (4.8 g, 22.1 mmol) and a trace of potassium iodide were then added, and the solution was heated at reflux for 30 h. The resulting mixture was poured into water and extracted with dichloromethane. After evaporation and drying, the crude product was recrystallized twice from ethanol. M.p. = 92 °C. Yield: 52%. IR: 3610 v(—OH), 1720 (C=O), and 2120 (N=N). Analysis for ethyl 4-[4-(6-hydroxyundecyl)phenylazo] benzoate (**2**) ($C_{26}H_{36}O_4N_2$, 440): Calc.: C, 70.91; H, 8.18; N, 6.36. Found: C, 70.95; H, 8.14; N, 6.37.

Ethyl 4-[4-(11-Methacryloyloxyundecyloxy)phenyl azobenzoyl-oxyl] Benzoate (M1)

Compound **2** (4.4 g, 10 mmol), triethylamine (3.1 g, 30 mmol), and a catalytic amount of hydroquinone were dissolved in distilled tetrahydrofuran (THF, 30 mL). The solution was cooled with an ice/salt bath and then methacryloyl chloride (2.1 g, 20 mmol), dissolved in distilled THF (10 mL), was added dropwise under vigorous stirring. The mixture was further stirred for 8 h at room temperature. After completing the reaction, the mixture was poured into cold water and the precipitate was filtered. The crude product was washed several times with water and then recrystallized twice from ethanol. M.p. = 95 °C. Yield: 85%.

^{1}H NMR ($CDCl_3$, δ in ppm): 1.21–1.53 (18H, CH_2), 1.55–1.58 (3H, CH_3), 1.67–1.70 (3H, CH_3), 4.05–4.45 (6H, OCH_2), 5.55 (1H, CH_2), 6.09 (1H, CH_2), 7.00–7.03 (2H, aromatic), 7.88–7.95 (4H, aromatic), 8.11–8.13 (2H, aromatic). IR: 3615 v(—OH), 2120 (N=N), 1720 (C=O), and 1640 (C=C). Analysis for ethyl 4-[4-(11-methacryloyloxyundecyloxy)phenyl azobenzoyloxyl] benzoate (**M1**) ($C_{30}H_{40}O_5N_2$, 508): Calc.: C, 70.87; H, 7.87; N, 5.51. Found: C, 70.68; H, 7.85; N, 5.53. ^{1}H-NMR spectrum of M1 can be found in the online version, which is available at www.interscience.wiley.com.

Synthesis of Diblock Copolymers

PMMA-Br Macroinitiator

Copper (I) bromide (Cu^IBr, 17.93 mg, 0.13 mmol), *N*,*N*,*N*′,*N*′,*N*"-pentamethyldiethyl entriamin (PMDETA, 43.33 mg, 0.25 mmol), and 1 mL of diphenyl ether in a 15-mL Schlenk flask were stirred using magnetic stirrer for 5 min at room temperature. Ethyl-α-bromoisobutyrate (EBiBr, 48.77 mg, 0.25 mmol) was added into the former mixture and then stirred for further 5 min at room temperatures. MMA (5 g, 50 mmol) in 3 mL diphenyl ether was added into the flask. The reactor was charged with nitrogen and then degassed by three freeze–thaw cycles. The reaction mixture was heated at 85 °C for 50 min. At the end of reaction, the flask was cooled using liquid nitrogen. The flask is opened and added 5 mL THF to terminate the polymerization. The reaction mixture was removed from the flask by a syringe and purified by passage through a silica column to remove the copper catalyst. The product was further purified by reprecipitation from cold hexane. The precipitated macroinitiator was filtered and dried under vacuum. M_n: 9645 g/mol, T_g: 93.1 °C. ^{1}H-NMR spectrum of PMMA-Br macroinitiator can be found in the online version, which is available at www.interscience.wiley.com.

*Diblock Copolymer PMMA-*b*-PAzoMA*

Cu^IBr (1.43 mg, 0.01 mmol), hexamethyl-triethylene-tetramine (HMTETA, 6.91 mg, 0.03 mmol), and 1 mL of anisole in a 15-mL Schlenk flask were stirred at room temperature for 5 min. Next, **PMMA-Br** (99.59 mg, 0.01 mmol) in 2 mL anisole was added into the flask and then stirred for further 5 min. After that 0.76 g of **M1** (1.5 mmol) in 3 mL anisole was

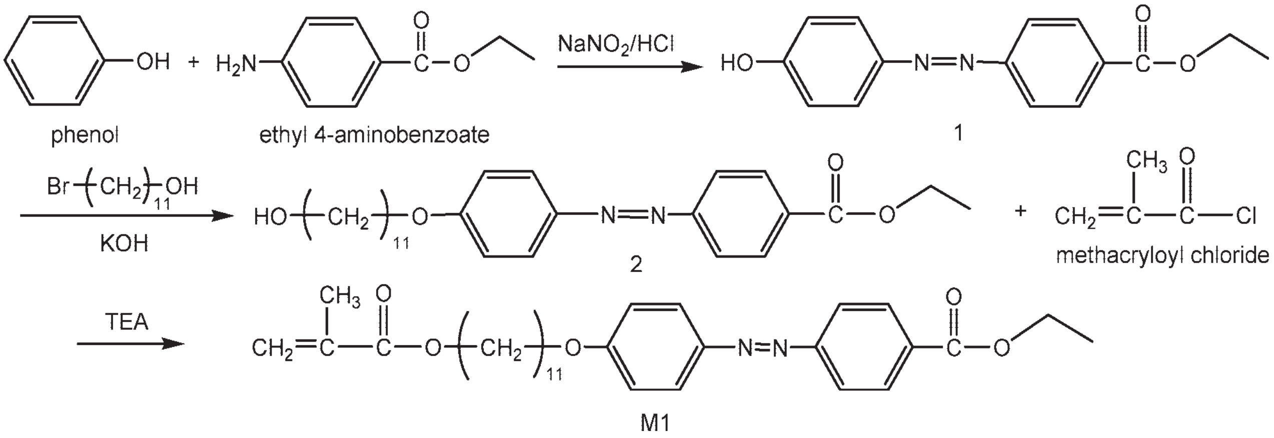

SCHEME 1 Synthesis of monomer **M1**.

added into the flask. The flask was tightly sealed with a rubber septum, degassed by three freeze–thaw cycles. The mixture was polymerized at 80 °C for 5 days. After polymerization, the reaction was terminated by adding 10 mL THF into the flask. The product was purified by passage through a silica gel column. The synthesized copolymer was reprecipitated from cold methanol and dried under vacuum. M_n: 27,561 g/mol, T_g: 59.7 and 95 °C. Both ^{1}H-NMR spectrum and thermal analyses of diblock copolymer **PMMA-*b*-AzoMA** can be found in the online version, which is available at www.interscience.wiley.com.

Self-Assembly of Diblock Copolymer PMMA-*b*-PAzoMA

Self-Assembly Formed in Solvent

PMMA-*b*-PAzoMA (0.2 mg) in 3.3 mg THF was added to 6.6 mg water. The mixture was stirred at room temperature for 30 min and then ultrasonically agitated for 30 min, after which it was put in an oven at 50 °C for 30 min. After cooling, one drop of the solution was set on a copper grid for TEM analysis. UV exposure was performed at 30 °C in THF/H_2O = 1:2 followed by standing at 30 °C for 2 h. The self-assembled sample was collected and dried for analysis. For visible light recovering exposure, samples were irradiated with a sunlight lamp at 30 °C in THF/H_2O = 1:2 and then kept at 30 °C for 1 day.

Thermal Annealing

PMMA-*b*-PAzoMA in toluene (1 wt %) was spin coated on a silicon substrate. The film thickness was controlled by controlling the spin-coating speed between 2000 and 4000 rpm for 30 s. After spin coating, the thin film was thermally annealed at 130 °C in a vacuum for 3 days. The morphology of the thermal annealed thin film was examined with AFM.

Solvent Annealing

Diblock copolymer **PMMA-*b*-PAzoMA** 5 wt % in THF was spin coated on a glass substrate at 2000 rpm for 30 s. After drying at room temperature in air atmosphere for 1 h, the spin-coated film was annealed in saturated acetone vapor for 4 h, and the resultant film sample was dried in vacuum. The morphology of the film sample annealed under various conditions was examined with AFM and SEM.

RESULTS AND DISCUSSION

Synthesis of Diblock Copolymer PMMA-*b*-PAzoMA

As shown in Scheme 1, ethyl 4-[4-(11-methacryloyloxyundecyloxy)phenyl azobenzoyloxyl] benzoate (**M1**) containing an azobenzene segment was synthesized. The molecular structure was confirmed using FTIR, NMR, and EA. To synthesize the amphiphilic diblock copolymer, as shown in Scheme 2, a macromolecular initiator was synthesized in the presence of a Cu^{I}Br catalyst. The synthesized macromolecular initiator, **PMMA-Br**, was used to synthesize the amphiphilic diblock copolymer **PMMA-*b*-PAzoMA**. The molecular weight and the T_g of the macromolecular initiator and diblock copolymer were estimated using GPC and dynamic scanning calorimetry (DSC), respectively. The results are shown in the Experimental section. Two significant glass transition temperatures of 59.7 and 95 °C were found in the **PMMA-*b*-PAzoMA** diblock copolymer, which are ascribed to the existence of the separated amphiphilic segments. Molecular weight distributions of macroinitiator **PMMA-Br** and copolymer **PMMA-*b*-PAzoMA** can be found in the online version, which is available at www.interscience.wiley.com.

Self-Assembly of Diblock Copolymer PMMA-*b*-PAzoMA in Solvent

To investigate the self-assembly of the synthesized diblock copolymer, **PMMA-*b*-PAzoMA** was dissolved in THF, and a certain amount of water was then added dropwise to the system. Weight ratios of THF/H_2O of 1:2, 1:1, and 2:1 were investigated. It was found that reverse micelles with spherical construction were obtained in the condition of 2 wt % diblock copolymer in THF/H_2O = 1:2. Under other conditions, however, no phase-separated constructs were found. In the case of 2 wt % copolymer, a reverse micelle should be formed. The hydrophobic **PMMA** segment could be enclosed inside the core of the spherical particles. Because of surface tension of the solvated surface, nanoparticles with spherical construction were formed. Furthermore, a 10 wt % polymer concentration caused the formation of bigger nanoparticles and the aggregation of phase-separated nanoparticles. High concentration of nanoparticles usually leads to aggregation.

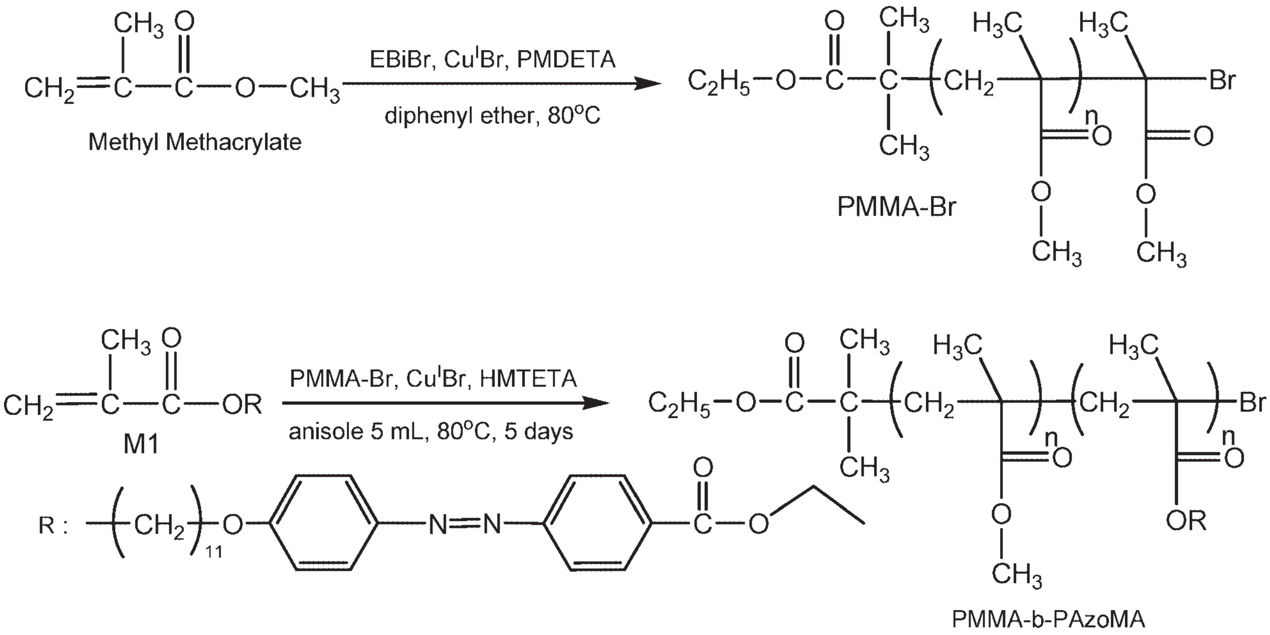

SCHEME 2 Synthesis of diblock copolymer **PMMA-*b*-PAzoMA**.

Interestingly, UV irradiation caused a deformation of the nanoparticles. As seen in Figure 1(a,b), after UV exposure, rod-like particles were formed. In addition, the rod-like particles were converted to spherical constructions when the sample was exposed to a sunlight lamp and then kept at 30 °C for 2 h with violent stirring. To describe the phenomena, UV–vis experiments of the diblock copolymer in THF were investigated. Figure 2(a,b) shows the results of the UV–vis experiments with the diblock copolymer in THF both before and after irradiation at 365 nm. As seen in Figure 2(a), the decrease in absorption around 365 nm is due to the E-Z isomerization of the azobenzene segment. It is known that UV-induced E-Z isomerization causes variations on configurational structure, polarity, and surface tension.[30,31] In our case, UV irradiation may cause the E-Z isomerization of the diblock copolymer **PMMA-*b*-AzoMA** leading to the change of both polarity and hydrophilicity of the segments. The variation in construction after UV irradiation, shown in Figure 1(b), could be ascribed to the variation of the hydrophilicity of pendant groups of the diblock copolymer. Hydrophilicity changes of the segments may cause a rearrangement of diblock copolymers. Figure 3 shows schematic representation of construction variation of self-assembly of the diblock copolymers before and after UV irradiation. After UV irradiation, hydrophilicity of the **PAzoMA** of the diblock copolymer could be changed leading to the aggregation of micelles and then the deformation of the aggregated spheres to rod-like construction. As seen in Figure 3, **PAzoMA** is located at the outer surface of nanoparticles. After UV irradiation, the hydrophilicity of **PAzoMA** segment may be increased leading to the aggregation of nanoparticles. The increase of solubility of **PAzoMA** in water may increase the mobility of the **PAzoMA** segment moving to the surface of the rod-like nanoparticle. Simultaneously, the stability of the rod-like particles is increased as well. These phenomena are quite similar to those reported for morphology variations in proper solvent before and after laser exposure.[32]

It is noteworthy that UV irradiation of the dry spherical diblock copolymer particles under an air atmosphere caused no significant change in construction. From the results of UV–vis analysis, UV irradiation caused significant variations on UV–vis spectra of the diblock copolymer film. The variation showed the progress of the E-Z isomerization in the film state. The stability of the spherical structure after UV exposure is attributed to the rigidity of the dry spherical particles. In case of the dry state, UV irradiation may still cause E-Z isomerization. However, the rigidity of the dry nanoparticles may restrict the rearrangement of diblock segments. As noted in the literature, the morphology of the nanoparticles was kept in poor solvent even after UV exposure.[33]

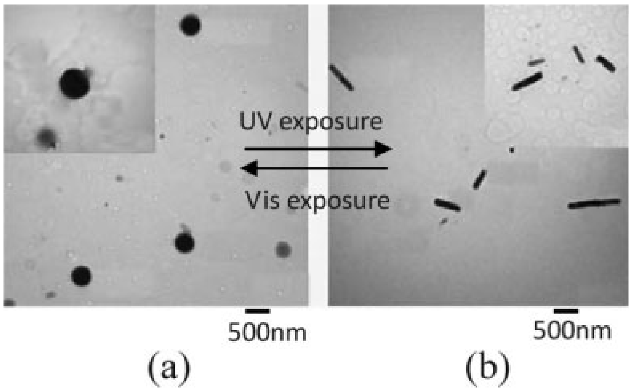

FIGURE 1 TEM images of self-assembled nanoparticles (a) before and (b) after UV exposure in THF/H_2O = 1:2.

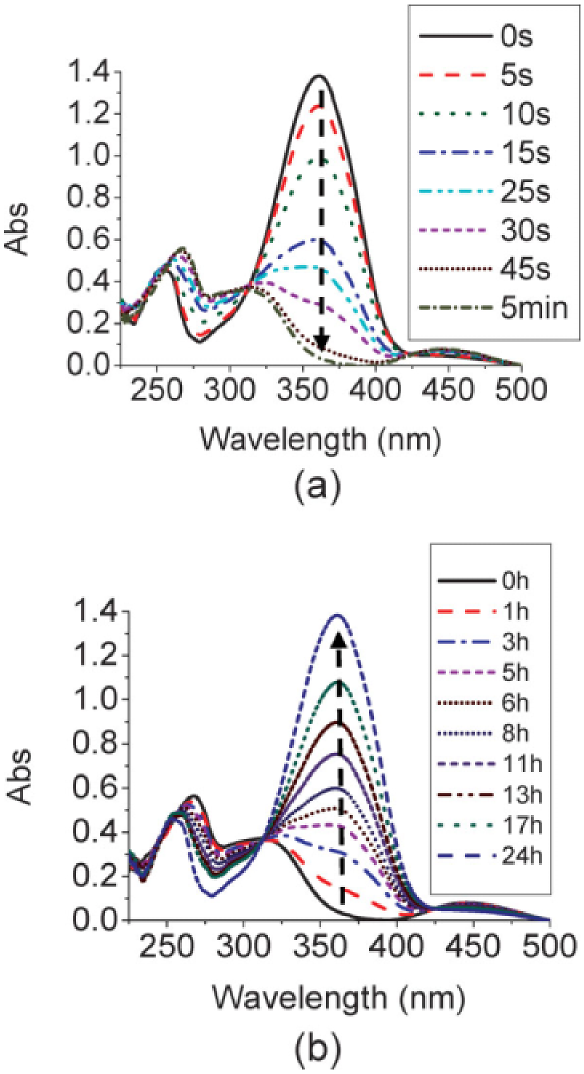

FIGURE 2 UV–vis spectra of **PMMA-*b*-PAzoMA** in THF (a) irradiated at 365 nm and (b) stability in the dark after 365-nm exposure.

Thermal Annealing of Diblock Copolymer

To investigate the thermal annealing of the diblock copolymer, **PMMA-*b*-PAzoMA** in toluene (1 wt %) was spin coated on a silicon substrate. After spin coating, the thin film was thermally annealed at 130 °C under vacuum for 3 days. The morphology of the thermally annealed thin film was examined with an AFM. Figure 4(a–c) shows the AFM morphology texture of 0.2 wt % copolymer with 4000 ppm, 0.2 wt % copolymer with 2000 ppm, and 1 wt % copolymer with 2000 ppm coated films, respectively. Figure 4(a–c) shows AFM height image before thermal annealing, and Figure 4(d–f) shows AFM height image after thermal annealing. As seen in Figure 4, after sufficient thermal annealing, phase separation occurred and leading to the formation of the microseparated patterns. Figure 5 shows a schematic representation for the formation of microphase separation. Heat-melted copolymers allow the rearrangement of both the hydrophilic and the lipophilic segments of the diblock copolymers. Because of the

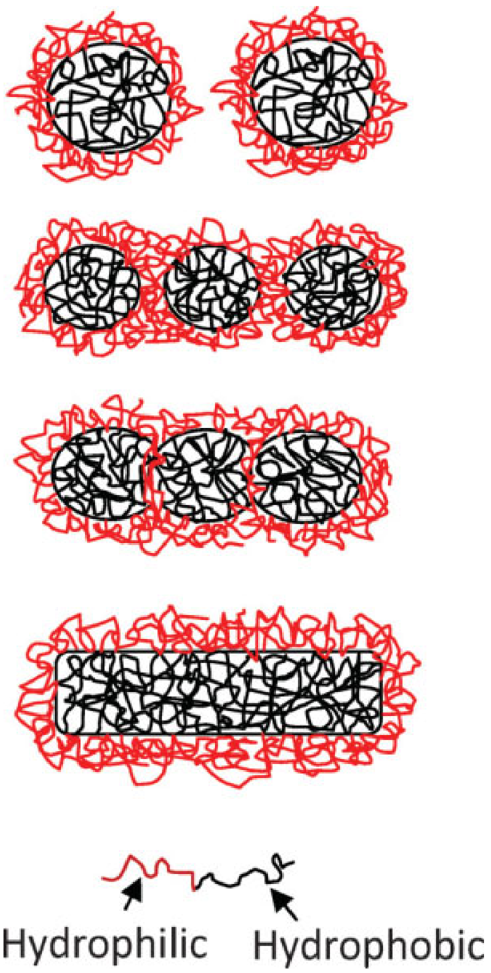

FIGURE 3 Schematic representation of the self-assembly of **PMMA-*b*-PAzoMA** in THF/H_2O = 1:2 (a) before and (b) after 365-nm exposure.

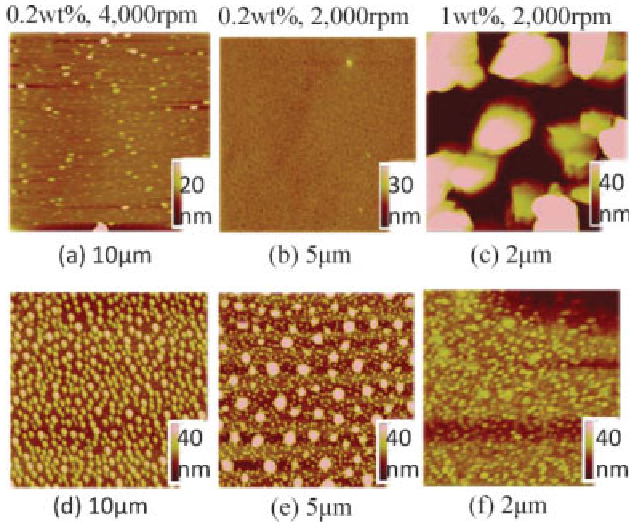

FIGURE 4 AFM height images of self-assembled **PMMA-*b*-PAzoMA** (a–c) "before" and (d–f) "after" thermal annealing.

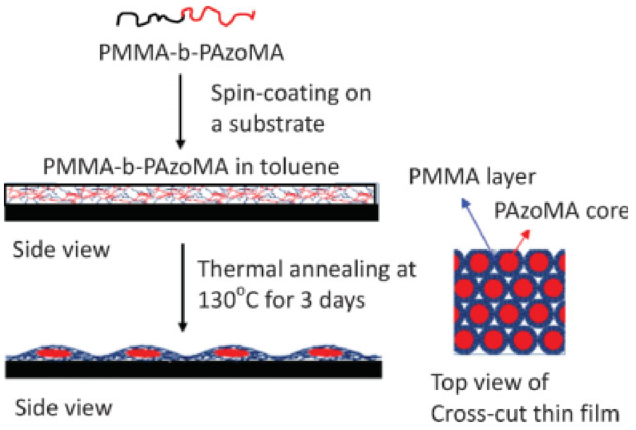

FIGURE 5 Schematic representation of self-assembled microphase separation of **PMMA-*b*-PAzoMA** after thermal annealing. [Color figure can be viewed in the online issue, which is available at www.interscience.wiley.com.]

hydrophilicity, **PMMA** segment interacted with hydrophobic silicon substrate. As seen in Figure 5, the domain patterns are attributed to the self-assembled **PAzoMA** core segments. The results are consistent with the AFM images shown in Figure 4. In case of high copolymer concentration film shown in Figure 4(c), the interaction from the silicon substrate on self-assembly of hydrophilic and hydrophobic segments may extremely decrease because of the increase of film thickness.[26]

Figure 6(a) shows the 3D AFM height image of the thermally annealed film. The inset photograph is the 2D image of the surface height pattern. The exact height of the domains is shown in Figure 6(b). Domains with various heights were formed on the thin film surface.

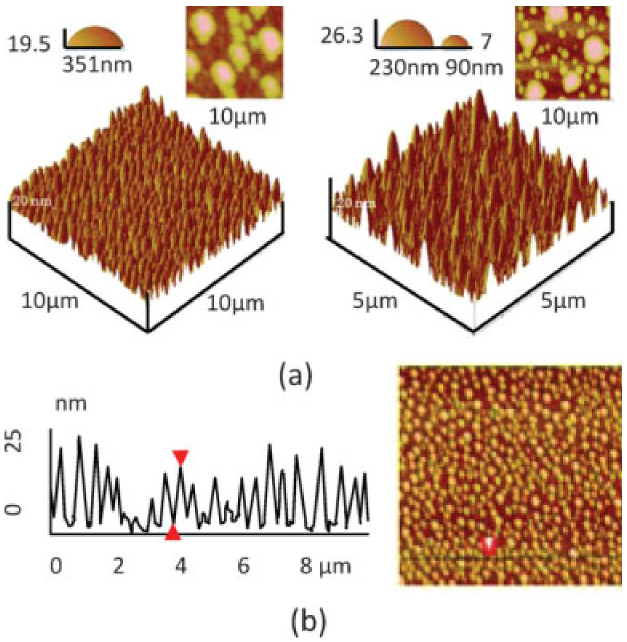

FIGURE 6 AFM (a) 3D height images and (b) height section analysis of thermally annealed **PMMA-*b*-PAzoMA**. [Color figure can be viewed in the online issue, which is available at www.interscience.wiley.com.]

Solvent Annealing of Diblock Copolymer Films

To investigate the solvent annealing of diblock copolymers, **PMMA-*b*-PAzoMA** was dissolved in THF and then was spin coated on a glass substrate. Solvent annealing of the thin film of the **PMMA-*b*-PAzoMA** diblock copolymer was performed at room temperature for 4 h in a closed vessel full of saturated acetone vapor leading to microphase separation. Figure 7(a–c) shows the mesoporous structures that were prepared by ambient drying, slow drying, and acetone annealing, respectively. In the case of ambient drying, the thin film was put in the air atmosphere. The slow drying of the thin film was performed in a closed vessel without solvent inside. For acetone annealing, the thin film was put in a closed vessel with a cup of acetone to saturate the atmosphere with acetone vapors for 4 h. As seen in Figure 7(a,b), the phase separation of the diblock copolymer is quite different from film annealed with acetone vapor. Sufficient acetone vapor treatment caused the microphase separation leading to the formation of the open pores. Figure 8 shows a schematic representation for the solvent annealing of the diblock copolymer. Hydrophobic **PMMA** segment may be dissolved in acetone and form separated domains. During the slow evaporation of acetone, the dissolved **PMMA** was pushed to the periphery of the domain. Solvent-dissolved **PMMA** segment may precipitate at the periphery of the open cores. As seen in Figure 7(a,b), in case of drying without saturated solvent vapor, bigger phase-separated domains were found because of lower amount of THF content in the system. The opened hole is somewhat complicated but can be ascribed to insufficient phase separation in the systems. In case of Figure 7(c),

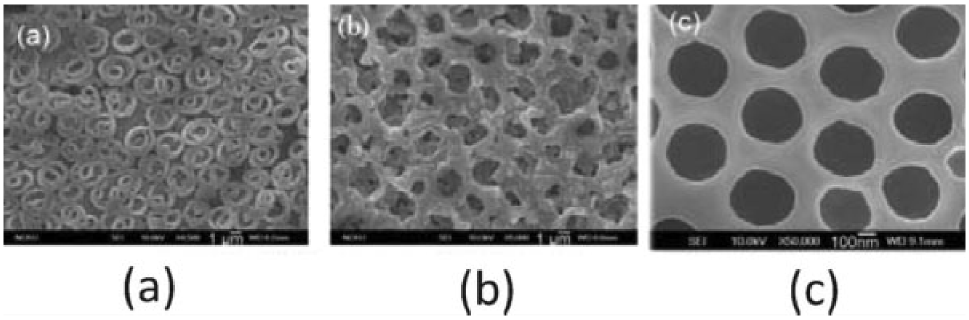

FIGURE 7 SEM images of **PMMA-*b*-PAzoMA** on a glass substrate prepared via (a) ambient drying, (b) slow drying, and (c) acetone annealing.

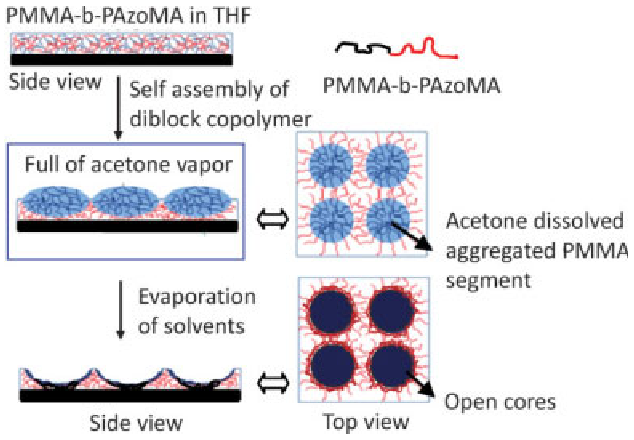

FIGURE 8 Schematic representation of the formation of mesoporous material in the **PMMA-*b*-PAzoMA** film via solvent annealing. [Color figure can be viewed in the online issue, which is available at www.interscience.wiley.com.]

sufficient acetone-dissolved **PMMA** may reach bottom substrate leading to the formation of through-hole after drying. 2D and 3D AFM height images of (a) 0.2 wt %, and (b) 1 wt % **PMMA-*b*-PAzoMA** diblock copolymer in toluene can be found in online version, which is available at www.interscience.wiley.com.

CONCLUSIONS

The amphiphilic diblock copolymer **PMMA-*b*-PAzoMA** was synthesized using ATRP. Reverse micelles with spherical construction were obtained using 2 wt % diblock copolymer in THF/H_2O = 1:2. Under alternating UV and visible light illumination, reversible changes in micellar structure between sphere and rod-like particles took place as a result of the reversible E-Z photoisomerization of the azobenzene segments in **PMMA-*b*-PAzoMA**. Microphase separation of the amphiphilic diblock copolymer in thin films was achieved through thermal and solvent aligning methods.

The authors thank the National Science Council (NSC) of the Republic of China (Taiwan) for financially supporting this research under Contract No. NSC 97-2221-E006-026.

REFERENCES AND NOTES

1 Zhang, D.; Hamilton, P. D.; Kao, J. L.; Venkataraman, S.; Wooley, K. L.; Ravi, N. J Polym Sci Part A: Polym Chem 2007, 45, 2569–2575.

2 Sriprom, W.; James, M.; Perrier, S.; Neto, C. Macromolecules 2009, 42, 3138–3146.

3 Tercjak, A.; Serrano, E.; Garcia, I.; Ocando, C.; Mondragon, I. Acta Mater 2007, 55, 6436–6443.

4 Wu, P. T.; Ren, G.; Li, C.; Mezzenga, R.; Jenekhe, S. A. Macromolecules 2009, 42, 2317–2320.

5 Tu, Y.; Wan, X.; Zhang, D.; Zhou, Q.; Wu, C. J Am Chem Soc 2000, 122, 10201–10205.

6 Glogowski, E.; Tangirala, R.; Russell, T. P.; Emrick, T. J Polym Sci Part A: Polym Chem 2006, 44, 5076–5086.

7 Bucholz, T. L.; Loo, Y. L. Macromolecules 2008, 41, 4069–4070.

8 Morikawa, Y.; Kondo, T.; Nagano, S.; Seki, T. Chem Mater 2007, 19, 1540–1542.

9 Ebara, K.; Shibasaki, Y.; Ueda, M. J Polym Sci Part A: Polym Chem 2002, 40, 3399–3405.

10 Scruggs, N. R.; Verduzco, R.; Uhrig, D.; Khan, W.; Park, S. Y.; Lal, J.; Kornfield, J. A. Macromolecules 2009, 42, 299–307.

11 Larson, D. J.; Long, A. K. P.; Ma, Y. Q.; Cerezo, A. Acta Mater 2004, 52, 2847–2862.

12 Tsang, E. M. W.; Zhang, Z.; Shi, Z.; Soboleva, T.; Holdcroft, S. J Am Chem Soc 2007, 129, 15106–15119.

13 Du, C.; Yun, J.; Dumas, R. K.; Yuan, X.; Liu, K.; Browning, N. D.; Pan, N. Acta Mater 2008, 56, 3516–3522.

14 Yu, Y.; Ouyang, C.; Gao, Y.; Si, Z.; Chen, W.; Wang, Z.; Xue, G. J Polym Sci Part A: Polym Chem 2005, 43, 6105–6115.

15 McHenry, M. E.; Laughlin, D. E. Acta Mater 2000, 48, 223–232.

16 Yu, H.; Iyoda, T.; Ikeda, T. J Am Chem Soc 2006, 128, 11010–11011.

17 Hafiz, H. R.; Nakanishi, F. Nanotechnology 2003, 14, 649–654.

18 Song, J.; Liu, Y. G.; Ma, J.; Xuan, L. Chin Phys Lett 2006, 23, 3285–3287.

19 Zhao, Y.; Qi, B.; Tong, X.; Zhao, Y. Macromolecules 2008, 41, 3823–3831.

20 Mu, Q. S.; Lu, J. R.; Ma, Y. H.; Banez, M. V. P.; Robinson, K. L.; Armes, S. P.; Lewis, A. L.; Thomas, R. K. Langmuir 2006, 22, 6153–6160.

21 Ding, L.; Mao, H.; Xu, J.; He, J.; Ding, X.; Russell, T. P.; Robello, D. R.; Mis, M. Macromolecules 2008, 41, 1897–1900.

22 Bo, Q.; Zhao, Y. Langmuir 2007, 23, 5746–5751.

23 Peris, S.; Tylkowski, B.; Ronda, J. C.; Garcia-Valls, R.; Reina, J. A.; Giamberini, M. J Polym Sci Part A: Polym Chem 2009, 47, 5426–5436.

24 Shibaev, V.; Medvedev, A.; Bobrovsky, A. J Polym Sci Part A: Polym Chem 2008, 46, 6532–6541.

25 Tong, X.; Zhao, Y. J Am Chem Soc 2007, 129, 6372–6373.

26 Qu, J.; Jiang, F.; Chen, H.; Sanda, F.; Masuda, T. J Polym Sci Part A: Polym Chem 2009, 47, 4749–4761.

27 Zeng, Q.; Li, Z.; Li, Z.; Ye, C.; Qin, J.; Tang, B. Z. Macromolecules 2007, 40, 5634–5637.

28 Liu, B.; He, Y.; Wang, X. Langmuir 2006, 22, 10233–10237.

29 Yager, K. G.; Tanchak, O. M.; Godbout, C.; Fritzsche, H.; Barrett, C. J. Macromolecules 2006, 39, 9311–9319.

30 Li, Y.; Deng, Y.; Tong, X.; Wang, X. Macromolecules 2006, 39, 1108–1115.

31 Tong, X.; Wang, G.; Soldera, A.; Zhao, Y. J Phys Chem B 2005, 109, 20281–20287.

32 Lee, H.; Char, K. Chem Mater 2005, 17, 2241–2246.

33 Deng, Y.; Li, N.; He, Y.; Wang, X. Macromolecules 2007, 40, 6669–6678.